[Cancer Biology & Therapy 5:7, 850-859, July 2006]; ©2006 Landes Bioscience

Research Paper

New Symmetrical Quinazoline Derivatives Selectively Induce Apoptosis in Human Cancer Cells

Elena Cubedo[1,*]
Lucia Cordeu[1]
Eva Bandres[1]
Amaia Rebollo[1]
Raquel Malumbres[1]
Carmen Sanmartin[2]
Maria Font[2]
Juan Antonio Palop[2]
Jesús Gacía-Foncillas[1]

[1]Laboratorio de Farmacogenómica; Área de Oncología; Centro de Investigación Médica Aplicada; Pamplona, Spain

[2]Departamento de Química Orgánica y Farmacéutica; University of Navarra; Pamplona, Spain

*Correspondence to: Elena Cubedo; Laboratorio de Farmacogenómica; Área de Oncología; Centro de Investigación Médica Aplicada (CIMA); Universidad de Navarra; Avda Pio XII 55; 31008-Pamplona, Espana; Tel.: +34.948.174900x1008; Fax: +34.948.174914; Email: ecubgil@alumni.unav.es

Received 12/07/05; Accepted 04/22/06

Previously published online as a *Cancer Biology & Therapy* E-publication: http://www.landesbioscience.com/journals/cbt/abstract.php?id=2841

KEY WORDS

apoptosis induction, quinazoline derivatives

ABBREVIATIONS

DMSO	dimethyl sulfoxide
PMSF	phenyl-methyl-sulfonyl fluoride
DTT	dithiothreitol
DAPI	4,6 diamidino-2-phenylindoline

ACKNOWLEDGEMENTS

The authors wish to express their gratitude to the University of Navarra Research Plan (Plan de Investigación de la Universidad de Navarra, PIUNA) for its financial support to the project. We thank the Center for Applied Genomics and the New Jersey Commission on Science and Technology for providing the Oligo 19K human Array.

ABSTRACT

In the search of new symmetrical derivatives with anticancer activity, we have looked for novel compounds able to induce a selective proapoptotic mechanism in cancer cells.

The potential antitumoral activity of several quinazoline derivatives was evaluated in vitro examining their cytotoxic effects against human breast, colon and bladder cancer cell lines. The IC_{50} value of the compounds that showed cytotoxic activity was calculated. These compounds were tested for their ability to induce caspase-3 activation and nuclear chromatin degradation.

Non-tumoral human cell lines were used to test the selectivity of the cytotoxic compounds against cancer cells. Several compounds showed no cytotoxicity in these cell lines.

Finally, JRF12 (2,4-dibenzylaminoquinazoline) was chosen as the best candidate and its mechanism of action was studied in more detail. A time dependent evaluation of apoptosis was performed in the three cancer cell lines, followed by an evaluation of the cell cycle regulation involvement that showed a decrease of cells in G_1 phase and increase of cells in G_2 phase before cell death.

2,4-dibenzylaminoquinazoline treatment produces few changes in the expression of genes as evaluated by using oligonucleotide microarrays and Q-RT-PCR assays.

In conclusion, 2,4-dibenzylaminoquinazoline is a promising anticancer drug showing cytostatic and apoptotic effects mainly in a transcription independent manner.

INTRODUCTION

Apoptosis is a highly regulated process important in embryonic and immune system development and tissue homeostasis.[1-4] This process is characterized by specific morphologic changes such as cell size compaction, chromatin condensation, DNA degradation, membrane blebbing and cell fragmentation into apoptotic bodies. The principal biochemical effectors of apoptosis are the caspases, that are synthetized as inactive zymogens that once activated cause the degradation of a variety of intracellular substrates and produce cell death.[5-10]

It is accepted that tumor growth may principally be due to reduced rates of cell death rather than to enhanced proliferation.[11-13] The process of apoptosis is now recognized as an important component of multi step carcinogenesis.[3,14-18] However, most cancer chemotherapy regimens make use of highly cytotoxic drugs that target proliferating cell populations. The non-discriminatory nature of these agents leads to severe side effects in normal cells with a high proliferative index, such as those of the gastrointestinal tract and bone marrow, thus limiting the effective dose of anticancer drug that can be administered.[19]

In the search of less toxic anticancer therapies, we have looked for novel compounds with anticancer activity based on a proapoptotic mechanism. In the design of these new structures, a general pattern has been adopted. These molecules have a central nucleus made up of an aromatic system, the ring of quinazoline, connected to two identical lateral arms consisting of an amine aliphatic chain of variable length and flexibility with or without heterocycles at the end of the chain.

Recently, we have described the synthesis of symmetrical derivatives as cytotoxic and apoptosis inducers.[20,21] In our search for new molecules with these activities, we have synthesized new derivatives of quinazoline 2,4-difunctionalized (unpublished results).

The central nucleus of quinazoline is involved in numerous biological activities, mainly in cancer, as the inhibition of folate metabolism and the inhibition of the tyrosine kinase activity, apoptosis induction and topoisomerase inhibition.[22-36]

The cytotoxicity of thirteen derivatives of quinazoline was evaluated. After confirmation of their implication in apoptosis and their lack of toxicity against non-tumoral human cell lines, 2,4-dibenzylaminoquinazoline (referred as JRF12) was chosen for the further study

of its mechanism of action because of its suitable apoptotic and cytotoxic profile.

MATERIAL AND METHODS

Cell lines and reagents. The five human cell lines were obtained from the American Tissue Culture Collection (Manassas, VA): HT29 (ATCC HTB 38) is a colon adenocarcinoma cell line, T24 (ATCC HTB-24) was obtained from urinary bladder cancer, MDA-MB-231 (ATCC HTB26) was established from adenocarcinoma of mammary gland , CRL8799 was obtained from breast epithelium (ATCC 184B5) and CRL11233 (ATCC THLE-3) from human liver.

HT29 and T24 cells were cultured in McCoys medium (Gibco), MDA-MB-231 in Leibovitz (Gibco), CRL8799 in MEG (Clonetics Corporation) and CRL11233 in BEGM (BEGM Bullet kit, Clonetics Corporation). These media were supplemented with 10% fetal bovine serum, penicillin (50 U/ml) and streptomycin (50 µg/mL). Cells were grown as monolayer in 175 cc flasks (Corning) and were incubated at 37°C in a humidified atmosphere containing 5% CO_2.

The evaluated compounds were dissolved in dimethyl sulfoxide (DMSO). The DMSO concentration was equalized in all media. In all cases, the concentration of solvent in culture medium did not exceed 0.5% (v/v).

Cytotoxicity study. Cytotoxicity was determined by using the neutral red assay as described by Lowik et Albas.[37] Ninety-six well flat bottom tissue culture plates (Microtest 96 Falcon, Becton Dickinson) were used for the experiments. Cells were resuspended in culture medium and 180 µL of cell suspension were added into each well. Cells were seeded at a density of 20 x 10^3/well, and then cultured for 14 h to assure similar attachment of all cells. Test agents or vehicle were then added to the cells in 20 µL of culture medium and incubated for 72 h. After washing with PBS, the cells were incubated at 37°C with neutral red during 1. 5 h. The dye was then extracted from the cells by the addition of 100 µL 0.05 M NaH_2PO_4 in 50% ethanol. Optical density was measured at 540 nm and 650 nm was used as a reference wavelength using a microtiter plate reader (Organon tecknica). The spectrophotometer was blanked on the first column of control wells containing solvent solution alone.[38,39]

Survival percentage was determined at the screening concentrations of 20 and 100 µM, using the survival percentage obtained with the cells treated only with the solvent (DMSO at 0.5%) as reference. The results are expressed as the average of triplicate assays. IC_{50} values were calculated for those compounds showing less than 50% survival in the cell lines at 100 µM concentration. This value was determined in triplicate by curvilinear regression analysis using the statistical program SPSS 11.0.

With regard to selectivity, cytotoxicity was determined in cell cultures of two non-tumoral lines, CRL-7899 and CRL-11233. The highest IC_{50} calculated in the three tumoral lines was selected as the test concentration for assays on non-tumoral cells. The IC_{50} obtained in MDA-MB-231 was evaluated in breast non-tumoral cells.

Colony formation assay. The different cell lines were seeded in six-well plates (Falcon, Becton Dickinson), cultured for 14 h and treated for 24 h with vehicle or with the IC_{50} of JRF12. Cells were then washed, fresh medium was added and incubation was continued for 7 days.

Cells were fixed with 100% methanol for 2 minutes and then stained with 1% toluidine blue. Colonies were counted and expressed as the percent survival relative to non-treated cells. Cell viability is expressed as medium ± SD of percent colonies formed 7 days after treatment, referred to control cells. Each experiment was performed by triplicate.

DNA fragmentation analysis. DNA fragmentation was measured at 48 h after treatment using the *Cell Death detection ELISA^{PLUS} kit* (Roche Diagnostics, Indianapolis, IN) exactly as recommended by manufacturer.[40-42]

In brief, the different cell lines were seeded in 96-well plates (2 x 10^4 cell/well). The cells were treated with various drugs at the IC_{50} for 48 h and then, after lysis in 200 µL lysis buffer for 30 min at room temperature; the lisates were centrifuged at 200 g for 10 min and after that, 20 µL from the supernatant were transferred to streptavidin-coated microtitre plates for analysis. Eighty microliters of the inmunoreagent containing monoclonal antibodies directed against DNA and histones were added to each well, and the plates were incubated on a shaker (300 r.p.m.) for 2 h at room temperature. The solution was then removed and the wells were rinsed three times with incubation buffer. One-hundred microliters of substrate solution were added to each well and after 10–20 min, the amount of citosolic mono- and oligonucleosomes (indicator of cell death) was determined spectrophotometrically at 405 nm using substrate solution as blank.

Measurement of caspase-3 activity. Detection was carried out by means of cytometry, using the *Active-Caspase-3 FITC Mab apoptosis kit* (Pharmingen), according to manufacturer, which evaluates the number of cells that contain the dimerized and activated form of caspase-3. The range of effective measurements for this enzyme was found to be between 14 and 48 h. Therefore, measurements were taken at 14, 24 and 48 h, and the obtained values were compared with those of control cells incubated without the test compounds. The test concentrations correspond to the IC_{50} values determined in the cytotoxicity assay. Cytometry was performed on a FACSCAN (Becton Dickinson).

Measurements of central caspases activity. Caspase-3 assays were carried out in plates of 9 cm diameter (Cellstar Greiner Bio-one). Cells were harvested by using a 0,25% trypsin/0,03 EDTA solution and then lysed with a buffer containing 1%Triton (100x); 50 mM Tris HCl pH8, 150 mM NaCl, 100 µg/mL PMSF and 1mM DTT. The soluble fraction of the cell lysate was then assayed for caspase-3 activity using Ac-DEVD-pNA, a colorimetric substrate for caspase-3. Eighty micrograms of protein were diluted in 50 µL of caspase-3 buffer containing 50 mM HEPES pH 7,4; 100 mM NaCl, 0,1% CHAPS, 10 mM DTT, 1 mM EDTA, 10% glycerol. Fifty microliters of the substrate, DEVD-pNA (Biomol) was added to a final concentration of 200 µM, and the plates were incubated for 24 h at 37°C and 5% CO_2. Levels of released p-nitroanitrile (pNA) were measured as absorbance at 405 nm. To confirm the correlation between caspase-3 activity and signal detection, control reactions were performed by addition of 1 µL of 1 mM DEVD-CHO (Biomol), an inhibitor of caspase-3, to the diluted protein samples followed by addition of the reaction buffer and incubation at 37°C for 30 min before adding the caspase-3 substrate.[6,43,44]

Morphological characteristics: Caspase-3 and nuclear staining. In order to evaluate nuclear morphology, cells were treated with the IC_{50} of the compound during the time of caspase-3 activation. Cells were washed with PBS, fixed with cold methanol at room temperature for 15 minutes, then washed with PBS and post-fixed and permeabilized with methanol/acetone during 10 minutes. After blocking with 1% BSA and 0,1% Tween 20 in PBS, 10 µg/mL of primary antibody against caspase-3 (Sta Cruz Biotechnology) (10 µg/mL)

Table 1 **IC_{50} values and goodness of curve fitting (R^2) of the compounds in three human tumor cell lines**

T24			HT29			MDA-MB-231		
Compounds	IC_{50} (μM)	R^2	Compounds	IC_{50} (μM)	R^2	Compounds	IC_{50} (μM)	R^2
JRF3	28.95	0.9	JRF3	18.92	0.9	JRF3	4.43	0.7
JRF4	19.32	0.6	JRF4	6.96	0.9	JRF4	1.09	0.8
JRF5	5.25	0.9	JRF5	3.57	0.9	JRF5	3.13	0.9
JRF6	23.33	1.0	JRF6	5.81	0.8	JRF6	7.56	0.9
JRF7	2.86	0.7	JRF7	2.3	0.7	JRF7	2.18	0.7
JRF8	3.45	0.8	JRF8	2.2	0.9	JRF8	4.18	0.8
JRF9	11.9	0.8	JRF9	3.78	0.8	JRF9	1.22	0.7
JRF10	3.32	0.9	JRF10	3.47	0.9	JRF10	10.36	0.9
JRF11	2.17	0.9	JRF11	1.64	0.7	JRF11	4.65	0.8
JRF12	5.96	0.8	JRF12	4.72	0.9	JRF12	1.79	0.7
JRF13	15.4	0.9	JRF13	4.42	0.7	JRF13	5.47	0.7
JRF14	6.41	0.7	JRF14	5.89	0.9	JRF14	4.26	0.7
JRF15	3.87	0.8	JRF15	2.88	0.9	JRF15	3.87	0.9

were applied using anti-IgG antibody as negative control at a dilution of 1:1000.

After overnight incubation at 4°C overnight the antibody was rinsed and washed with PBS (1% BSA), then treated 60 minutes with antirabbit antibody at 1:1000 dilution (Jackson, Inmunoresearch laboratories, INC). Further, it was washed with PBS and stained with 4'6-diamidino-2-phenylindoline (DAPI) 1:10 dilution in PBS and glycerol. The nuclear morphology was visualized using fluorescence microscopy.

Specific inhibition of caspases. To determine the involvement of caspase-8 and caspase-9 in proapoptotic activity, a specific inhibitor of each caspase, Z-IETD-FMK and Z-LEHD-FMK respectively and a general caspase inhibitor (Z-VAD-fmk) were added 4 hours before treating with JRF12; all of them were purchased from Calbiochem (SanDiego, CA, USA). Vehicle DMSO at a final concentration of 0.5% was included as control. The effect of these inhibitors was estimated by measuring cytotoxicity with neutral red assay as described above. The experiment was performed treating cells with the caspase inhibitors (100 μM) and 1.5 x IC_{50} JRF12 during 48 h, or with 25 μM of caspase inhibitors and 2 x JRF12 IC_{50} during 24 h.

Cell cycle analysis. Single cell suspensions were obtained from cell monolayers as follows. First, cells were washed with PBS and then incubated 5 minutes with trypsin. Cells were collected from the dishes in the presence of PBS and were washed and resuspended in 1 mL of PBS. For cell cycle analysis, cells were fixed with ice-cold 100% ethanol and incubated at 4°C for 15 minutes. Cells were then resuspended in 125 μL of ribonuclease type IIA and incubated at 37°C for 15 minutes, then resuspended in 125 μL of propidium iodine (25 μg/mL) and incubated at room temperature for 30 minutes in obscurity. Before DNA content analysis cells were filtered by 40 μm nylon mesh filter. The analysis was performed on a Becton Dickinson FACScan flow cytometer using the CellQuest Software. All the results were obtained from three independent experiments.

Oligonucleotide microarrays. The different cell lines were seeded at a rate of 8 x 10^6 per flask, grown during 14 h and then were treated with DMSO (vehicle control) or IC_{50} of JRF12 for two different times (caspase-3 activation and DNA fragmentation). The rationale for choosing these time points was to capture gene expression profile of early response genes, and those involved in the induction of apoptosis.

Total RNA from each sample was isolated using the *RNeasy Midi Kit and RNAse-free DNAse Set* (QIAGEN, Valencia, CA) according to the manufacturer's protocols. The RNA concentration was calculated by spectrophotometry and it was adjusted to 1 μg/μL. Quality control of RNA integrity was performed by electrophoresis on a 2% agarose gel using ethidium bromide staining.

The *3DNA Submicro Oligo Expression Detection Kit* (Genisphere) was used to perform the reverse transcription as recommended by manufacturer; afterwards, cDNA was prehybridized with the fluorescent reactive 3DNA. Then, the samples were hybridised to the slides from the centre for Applied Genomics of the University of New Jersey. These slides contain 18.861 oligos. After overnight hybridization at 50°C in a slide cassette (Telechem, Sunnyvale, CA), slides were washed sequentially in a series of solutions with increasing stringency: 2x SSC, 0,2% SDS during 5 min at room temperature; 2x SSC 0,2% SDS, 15 min, 42°C; 2X SSC, during 10 min at room temperature; and finally 0,2 × SSC during 10 min at room temperature.

To remove the systematic bias caused by the chemical difference between Cy3 and Cy5, each microarray study was performed twice using dye-swap.

Microarray data acquisition, normalization and analysis. The hybridized slides were scanned with the GMS 418 scanner (Genetic Microsystems, Woburn, MA). After image acquisition, the scanned images were imported into "ImaGene 4.1" software (BioDiscovery) to quantify the signal intensities. Data from spots not recognized by the Imagene analysis software (empty, poor and negative spots) were excluded from further considerations. We also removed data from spots identified as visually flawed. The fluorescent median signal intensity for each spot was calculated using local median background subtraction. Data were normalized using Global mean, Dye-swap Pairs normalization and Dye Swap Fix filter 1.5 with the program ArrayNorm 1.7 (Graz, Austria).[45] Log ratios above 1.7 or below -1.7 were considered as differential expression.

The data discussed in this publication have been deposited in NCBI's Gene Expression Omnibus (GEO, www.ncbi.nlm.nih.gov/geo/) and are accessible through GEO Series accession number GSE3329.

Quantitative RT-PCR. The same RNA prepared for microarray analysis was also used for real-time RT-PCR. 2 μg of total RNA were used to generate cDNA using the Taqman Reverse transcription Reagent Kit (PE Applied Biosystem, Foster city, CA) according to the manufacturer's protocol. Each cDNA sample was analysed in triplicate using the Abiprism7700 sequence detector (PE Applied Biosystems). Quantitative assessment of DNA amplification was performed using Taqman Master Mix (PE Applied biosystems). The Q-RT-PCR reactions were carried out in a total volume of 25 μl containing 5 μg of cDNA, 2,5 μL of the corresponding Assay on Demand (PE Applied Biosystems), 5 μL of water and 12.5 μL of 2x Universal PCR Master Mix. The conditions for thermal cycling were: 2 min 50°C, 10 min 95°C and 40 cycles of 95°C 15 min and 60°C 1 min. The housekeeping gene coding for β-2 microglobuline was used as endogenous control transcript.

Fold induction was calculated using the formula $2^{-\Delta\Delta Ct}$, were ΔCt = target gene Ct - "housekeeping gene" Ct, and ΔΔCt is based on the mean of respective controls. The Ct value is determined as the cycle at which the fluorescent signal emitted is significantly above background levels and it is inversely proportional to the initial template copy number.

Statistics. Data are presented as mean ± SD. IC_{50} values were analysed using a non-linear regression model. Non-parametric or parametric test were performed according to the normality test results. The SPSS 11.0 software was used for all statistical analyses.

RESULTS

Cytotoxicity. The cytotoxic activity of the synthesized quinazoline derivatives was determined in the three human cancer cell lines at 100 and 20 μM using the neutral red assay. All compounds were toxic in the three cell lines tested. The IC_{50} values of the compounds are shown in Table 1. We used camptothecin as reference substrate, its IC_{50} values were 0.291 μM in MD-MB-231; 0,014 μM in HT-29 and 0.006 μM in T-24.

All the compounds showed good activity against all cancer cell lines tested, with IC_{50} values no higher than 30 μM.

Apoptosis detection: Caspase-3 activity and DNA fragmentation. Once the cytotoxicity of the compounds was verified, the induction of apoptosis was studied. Caspase-3 is believed to serve as a general mediator and is activated early during apoptosis. It is often considered the key executioner apoptosis because of its ability to cleave a vast array of proteins.[5,46] The levels of this enzyme were measured at 14, 24 and 48 h. Five compounds activate caspase-3 in T24: JRF7, JRF8, JRF9, JRF10 and JRF12, and three in the HT29 cell line: JRF9, JRF10 and JRF11. For MDA-MB-231 cells the cytometry could not be performed due to the obstruction of the cytometer by the conglomerates these cells form in suspension.

The ability to induce DNA fragmentation in cell culture was tested using the *Cell Death detection Elisa Plus Kit* (Roche). The level of DNA degradation measured in the control culture was considered as 1. Five compounds showed remarkable induction of DNA degradation in T24: JRF3, JRF5, JRF13, JRF14 and JRF15. Six compounds induced significant DNA degradation in HT-29: JRF4, JRF5, JRF9, JRF12, JRF13 and JRF15. JRF5 and JRF12 showed this effect in MDA-MB-231. Only JRF5 was able to induce DNA degradation in the three cancer cell lines while JRF12 and JRF15 showed this effect in two cell lines.

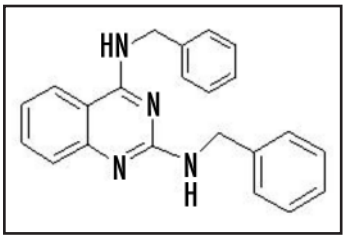

Figure 1. The structural formula of JRF12 (2,4-dibenzylaminoquinazoline).

Selectivity. In order to study the degree of selectivity, the cytotoxicity of the compounds was tested in cell cultures of two non-tumoral lines: CRL-8799 and CRL-11233, selected because they constitute an in vitro model often used for pharmacotoxicological studies.[47] Survival values were between 90% and 100% for JRF3, JRF4, JRF6, JRF8 and JRF12 in CRL8799 at IC_{50} (Table 2).

The best values were obtained with the compounds JRF8, JRF12 and JRF15. At the highest concentration, JRF8 was not toxic in CRL-8799 but toxic in CRL11233; inversely JRF15 was not toxic in CRL11233, being toxic in CRL8799. The compound JRF12 was not toxic in either cell line.

JRF12, 2,4-dibenzylaminoquinazoline (Fig. 1), was selected due to its ability to induce at least one apoptotic event in the three tumor cell lines tested, being not citotoxic for the non-neoplasic cell lines.

Colony formation assay. We evaluated the effects of JRF12 on cell growth by colony formation assay. The colony number decreased to 18 ± 0.04% and 11 ± 0.04% in T24 and HT29 cells respectively, and a viability of 72 ± 0.02% was observed in MDA-MB-231.

There is a remarkable inhibition of cell growth both in T24 and in HT29, but these effects are less severe in MDA-MB-231, in which the viability decreases only a 28%.

Table 2 **Selectivity of the evaluated compounds in two non-tumoral cell lines**

	Survival values in CRL8799				Survival values in CRL11233	
Compounds	IC_{50} MDA_MB_231		Higher IC_{50}		Higher IC_{50}	
CT	100%	0,1	100%	0,1	100%	0,1
JRF3	N.T.	0,1	0%	0,0	66%	0,6
JRF4	N.T.	0,2	4%	0,1	1%	0,0
JRF5	73%	0,0	4%	0,1	5%	0,1
JRF6	N.T.	0,0	2%	0,1	0%	
JRF7	78%	0,8	11%	0,1	23%	0,2
JRF8	87%	0,0	87%	0,0	2%	0,0
JRF9	64%	0,6	6%	0,1	11%	0,2
JRF10	11%	0,1	11%	0,1	1%	0,0
JRF11	0%		0%	0,0	0%	
JRF12	N.T.		89%	0,0	N.T	
JRF13	70%	0,6	13%	0,1	33%	0,2
JRF14	0%		0%		0%	0,0
JRF15	0%		0%		N.T	

The results are shown as percentage accompanied of their respective R2.

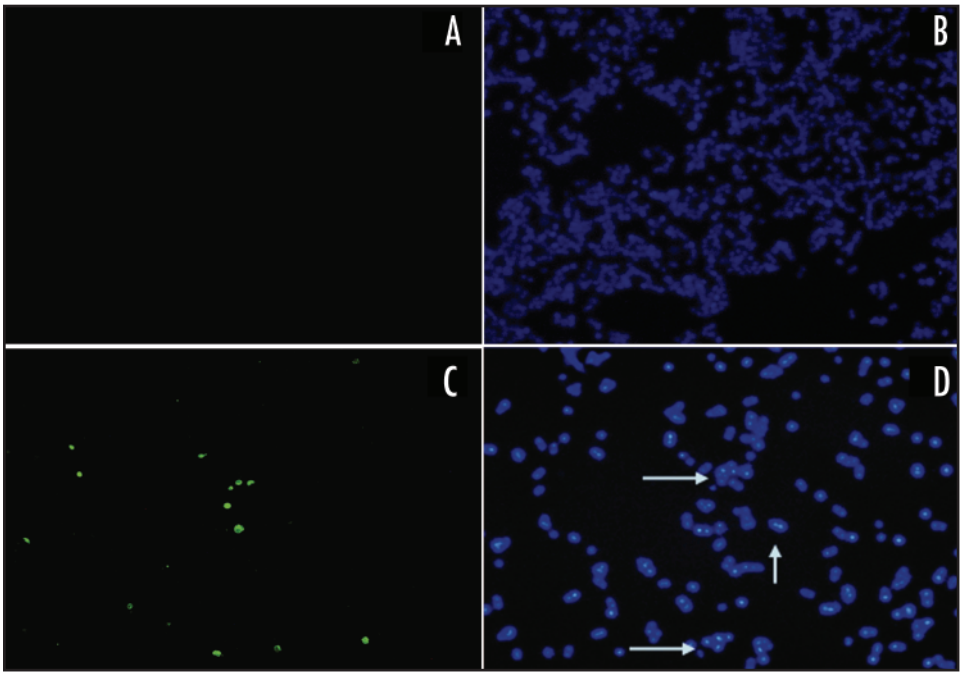

Figure 2. Inmunofluorescence studies. Cells were cultured in the presence or absence of IC_{50} doses JRF12 for the time of caspase-3 activation before cells were fixed, incubated with caspase-3 antibody and stained with DAPI. Stained nuclei were then observed under fluorescent microscope. (A) Control cells with caspase-3 antibody. (B) Control cells with DAPI. (C) Cells treated and incubated with caspase-3 antibody. (D) Cells treated and stained with DAPI.

Table 3 **Effects of 2,4-dibenzylaminoquinazoline on cell cycle progression in HT29 and T24 cell lines**

A. HT29

	Sub-G1	G0/G1	S	G2/M
Control	1%	51%	10%	37%
6 h	2%	43%	15%	39%
12 h	2%	45%	8%	44%
18 h	2%	37%	5%	56%
24 h	6%	33%	6%	55%
30 h	7%	39%	4%	50%

B. T24

	Sub-G1	G0/G1	S	G2/M
Control	6%	50%	14%	30%
6 h	8%	47%	11%	34%
12 h	9%	44%	12%	35%
18 h	24%	36%	13%	27%
24 h	26%	38%	12%	23%
30 h	35%	27%	10%	28%

Cells were treated with IC_{50} dose of 2,4-dibencilaminoquinazoline for different times and analyzed by flow cytometry and the percentages of distribution of cell cycle were reported. Data are representative of three independent experiments.

Time course analysis of JRF12 apoptosis induction: DNA fragmentation and caspase-3 activation. In T24 cells treated with the IC_{50} dose of JRF12, DNA degradation began at 14 h and reached its maximum value at 28 h. This effect did not disappear until 38 h. The effect is slower in HT29, where it began at 24 hours reaching its highest value at 28 hours and did not finish until 44 hours. In the breast cell line, MDA-MB-231, we have only found significant differences at 16 hours. This result agrees with those found for all the compounds evaluated previously that showed a minimal effect in this cell line.

We used a colorimetric enzymatic assay to measure changes of caspase-3 activity between extracts prepared from control and JRF12 treated cells. Cells were treated with their corresponding IC_{50} at different times. JRF12 stimulates caspase-3 like activity in the three cell lines. In a time course study, at the IC_{50} dose of JRF12 caspase-3 activity reached a peak after 18 h of treatment in T24, while in HT29 this peak appeared at 24 h and after 10 hours in MDA-MB-231, which correlated with the inmunofluorescence results.

The above results indicate that caspase-3-like proteases were activated in response to treatment with JRF12. To confirm that the obtained signal was due to caspase-3-like protease activity, caspase-3 inhibition by DEVD-CHO was evaluated showing a complete decrease of activation.[6,44,48]

Inmunofluorecence studies. We also examined the activation of caspase-3 by inmunofluorescence and the nuclear morphology of dying cells with the fluorescent DNA-binding agent, DAPI. As shown in Figure 2, after IC_{50} treatment during the time of caspase-3 activation in each cell line, T24 cells clearly exhibited nuclear segmentation and chromatin condensation, classical features of apoptosis, and activation of caspase-3. No altered nuclear morphology was observed in control cells treated with the vehicle. Thus, this result confirms that JRF12 cytotoxicity is mediated through the initiation of the apoptotic program, corroborating the results obtained previously.

Effect of caspase inhibitors on JRF12-induced apoptosis. To determine the involvement of caspases 8 and 9 in the cell death induced by JRF12, and therefore the pathway the compound is activating, we examined the effects of specific inhibitors, Z-IETD-FMK for caspase-8 and Z-LEHD-FMK for caspase-9. We moreover examined the effects of the general inhibitor of caspases Z-VAD-FMK on cell viability (Fig. 3). It was evaluated at 24 and 48h.

As measured by cell viability, all the caspase inhibitors assayed prevented induction of apoptosis after treatment with JRF12. The general caspase inhibitor, Z-VAD-FMK, inhibits cell death in the three cell lines evaluated, confirming that caspases are implicated in cell death induced by JRF12. Caspase-8 and caspase-9 inhibitors also inhibit cell death. The effect of caspase-8 is greater than that of caspase-9 in the three cell lines tested, suggesting that JRF12 activates cell death by caspase-8.

Cell cycle progression. Flow cytometry analysis showed that the treatment with IC_{50} JRF12 for 30 h induces a progressive time-dependent accumulation of cells in G_2/M in HT29 cell line (Table 3). G_2 cell population increased from 37% in the control to 55% in the presence of the IC_{50} dose of JRF12. In the mean time, cells in G_1 and S phase gradually decreased; G_1 percentage was 51% at time 0 and decreased to 33% at 24 hours.

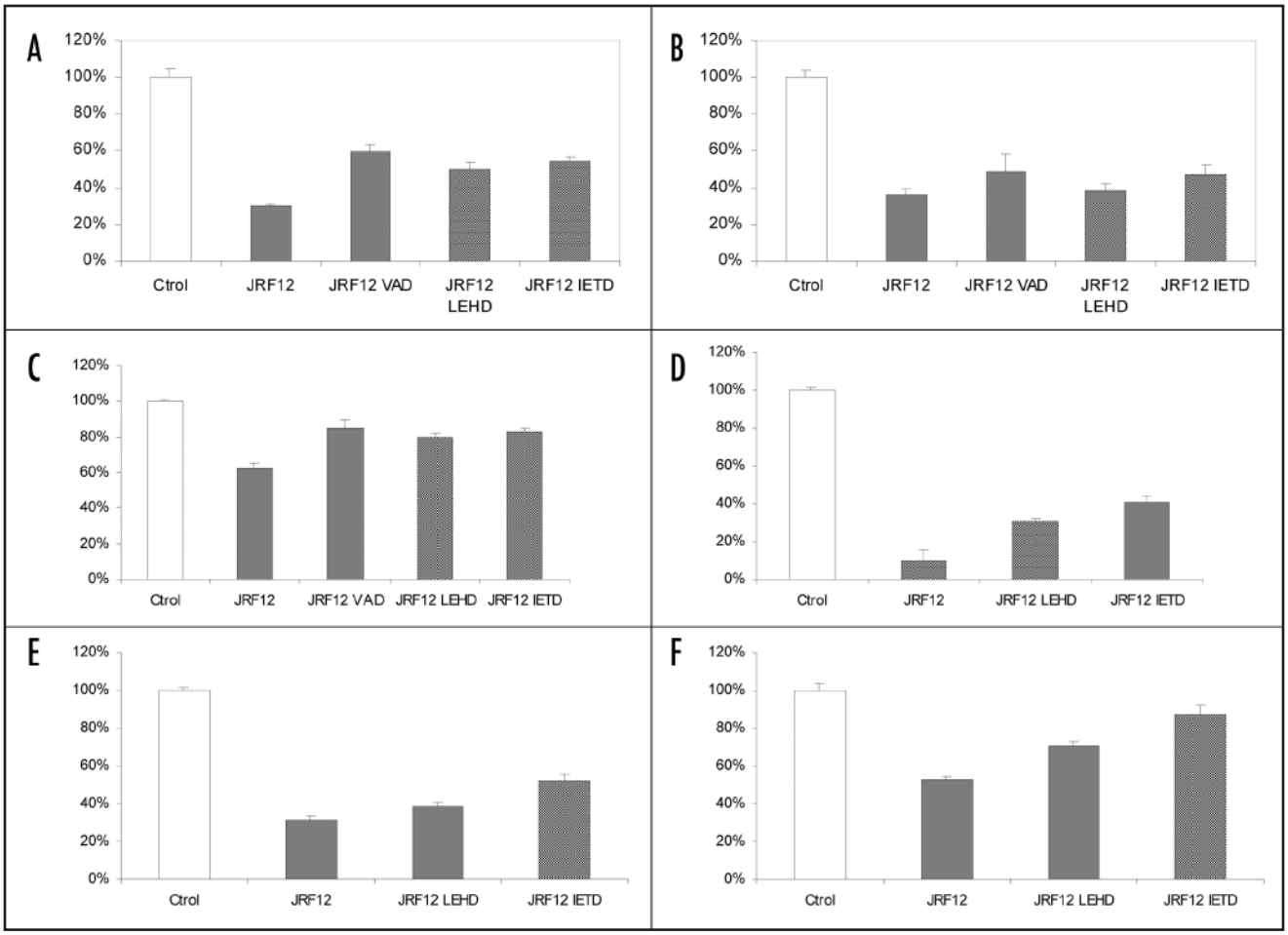

Figure 3. Number of viable cells 24 and 48 h after exposure to, respectively, 1,5 and 2 x IC_{50} doses JRF12 in presence of caspase inhibitors. (A) Cell viability after treatment with each inhibitor in T24 for 48 h. (B) Cell viability after treatment with each inhibitor in HT29 for 48 h. (C) Cell viability after treatment with each inhibitor in MDA-MB-231 for 48 h. (D) Cell viability after treatment with each inhibitor in T24 for 24 h. (E) Cell viability after treatment with each inhibitor in HT29 for 24 h. (F) Cell viability after treatment with each inhibitor in MDA-MB-231 for 24 h.

In T24 cells (Table 3), there was a decrease in the number of cells in G_1, but not an increase in the number of cells in G_2. Nevertheless, a characteristic hypo-diploid DNA content peak (sub-G_1) can be easily detected at 24 h, time at which we have detected activation of apoptosis previously. The slight decrease in the G_2/M cell population observed at 24 and 30 h could be explained by a decrease in the cell G_2 phase entering due to apoptosis.

Microarrays analysis. To determine whether gene expression was affected by JRF12 treatment in the three cell lines, we used oligonucleotide arrays. The different cell lines were treated with the IC_{50} value of JRF12 for two different times, the first corresponding to caspase activation and the second to DNA fragmentation.

T24 cells were treated during 20 and 24 hours. At 20 h, 2 genes were upregulated in treated cells, while 1 gene was downregulated. At 24 h 2 genes were upregulated and 3 downregulated at the second time (Table 4).

HT29 cells were treated for 24 and 28 hours. At 24 h, a total of 14 genes were upregulated in treated cells and 15 genes were downregulated. At 28 h, 10 genes were upregulated and 18 downregulated (Table 4).

MDA-MB-231 cells were treated for 9 and 24 h. 8 genes were upregulated while 11 were downregulated at the first of the time points, and 7 genes were upregulated and 11 genes were downregulated at the second time point (Table 4).

The limited number of genes with altered expression suggests that JRF12 may mediate its effects via posttranscriptional mechanisms.

Microarray validation. Quantitative RT-PCR analysis was used to confirm the results of the microarray experiments. The expression of different genes such as ABCB8 in T24, PDCD2 and ITGAL in MDA-MB-231 and RFP2 and ITGB4P in HT29 was evaluated (Fig. 4). The obtained results were consistent with the microarray data.

DISCUSSION

In this study, our aim was to find a new chemical compound able to induce selective apoptosis in human cancer cells. We synthesized novel symmetrical compounds based on a general pattern derived from a nucleus of quinazoline. These compounds were tested for cytotoxicity against three human cancer cell lines: breast (MDA-MB-231), colon (HT-29), and bladder (T24). All the compounds showed anticancer activity against all of the cell lines tested, with IC_{50} values in the low micromolar range. Some compounds exhibited great ability inducing apoptosis, being able to promote caspase-3 activation and DNA degradation. Among them, 2,4-dibenzylaminoquinazoline was the compound showing better selectivity for cancer cells, without toxicity against the non-tumoral cell lines CRL-7899 and CRL-11233.

Table 4 **Genes upregulated and down-regulated in the three cancer cell lines exposed to the IC_{50} of JRF12 at two times**

A. HT29		
Genebank	**Symbol**	**Description**
		Caspase-3 activation
Upregulated		
AK025684		Homo sapiens cDNA: FLJ22031 fis, clone HEP08734
NM_018246		Homo sapiens hypothetical protein FLJ10853 (FLJ10853),
AF164963		Homo sapiens tumor antigen NA88-A pseudogene, complete sequence
NM_018026	PACS1	Homo sapiens phosphofurin acidic cluster sorting protein 1
Z36816		H.sapiens (xs164) mRNA, 400bp
AF147368		Homo sapiens full length insert cDNA clone YB64D10
AJ224170		Homo sapiens mRNA containing U19H snoRNA
NM_012244	SLC7A8	Homo sapiens solute carrier family 7
U61095		Human NTera2D1 cell line mRNA containing L1 retroposon, clone P6
NM_001433		Homo sapiens ER to nucleus signalling 1
AB007859		Homo sapiens mRNA for KIAA0399 protein
AJ243673		Homo sapiens cDNA from NICE-2 gene
NM_016385	CYLD	Homo sapiens cylindromatosis
Downregulated		
D17207		Human HepG2 3' region MboI cDNA, clone hmd3e08m3
AK026753		Homo sapiens cDNA: FLJ23100 fis, clone LNG07523
NM_005798	RFP2	Homo sapiens ret finger protein 2
AF131781		Homo sapiens clone 24901 mRNA sequence, complete cds
AL109684		Homo sapiens mRNA full length insert cDNA clone EUROIMAGE 27080.
NM_015485	RWDD3	Homo sapiens RWD domain containing 3
NM_013275		Homo sapiens cDNA FLJ11564 fis, clone HEMBA1003220
AK023929		Homo sapiens cDNA FLJ13867 fis, clone THYRO1001262
AF086501		Homo sapiens full length insert cDNA clone ZE01F07.
AK026942		Homo sapiens cDNA: FLJ23289 fis, clone HEP10028
NM_003436	ZNF135	Homo sapiens zinc finger protein 135
NM_006733	FSHPRH1	Homo sapiens FSH primary response
NM_013339	ALG6	Homo sapiens asparagine-linked glycosylation 6 homolog
U12028		Human Cri-du-chat mRNA, partial sequence
AK021778		Homo sapiens cDNA FLJ11716 fis, clone HEMBA1005232
NM_001036	RYR3	Homo sapiens ryanodine receptor 3
		DNA degradation
Upregulated		
AK026984		Homo sapiens cDNA: FLJ23331 fis, clone HEP12664
AK022471		Homo sapiens cDNA FLJ12409 fis, clone MAMMA1002895
NM_000212	ITGB3	Homo sapiens integrin, beta 3
AB024518		Homo sapiens mRNA for DVS27-related protein, complete cds
NM_003522	HIST1H2BF	Homo sapiens histone 1, H2bf
AK021626		Homo sapiens cDNA FLJ11564 fis, clone HEMBA1003220
AF086176		Homo sapiens cDNA FLJ13867 fis, clone THYRO1001262
NM_015972	POLR1D	Homo sapiens polymerase (RNA) I polypeptide D, 16kDa
U50537		Human BRCA2 region, mRNA sequence CG033
AK022856		Homo sapiens cDNA FLJ12794 fis, clone NT2RP2002041
Downregulated		
M73837	MRF-2	Homo sapiens modulator recognition factor 2
NM_002212	ITGB4BP	Homo sapiens integrin beta 4 binding protein
AB037804		Homo sapiens mRNA for KIAA1383 protein

The data reported here also demonstrate that 2,4-dibenzylaminoquinazoline is able to induce an apoptotic response with caspase-3 activation and DNA degradation in at least two cell lines. Both events occurred faster and earlier in T24 cells than in HT29 cells. There is a lower induction of apoptosis in MDA-MB-231 although cell toxicity is present. There are several possible explanations for the discrepancies between the sensitivity of the MDA-MB-231 to JRF12 when measured cell cytotoxicity and realized apoptosis assays: the obtained results suggest that while they appear to be less sensitive to the apoptosis-inducing effects of 2,4-dibenzylaminoquinazoline, MDA-MB-231 cells are somewhat more sensitive to this compound in terms of the absolute decrease in cell number observed in the cytotoxic assays. This implies that additional mechanisms, other than apoptosis, may work in concert with the apoptotic program to cause cell death in this cell line. The differences in the type of cell death induced by 2,4-dibenzylaminoquinazoline may be linked to the diverse types of genetic alterations that occur in the different tumor cell lines.

By determination of cell cycle progression in response to 2,4-dibenzylaminoquinazoline, an increase of G_2 /M arrest was detected in HT29, while in T24 we observed cell death instead of cell cycle arrest. Our study shows that HT29 cells exposed to the IC_{50} dose of 2,4-dibencilaminoquinazoline undergo prolonged but transient G_2/M arrest followed by G_2 to M progression and after that cell death or G_1 progression. Whereas T24 cells exposed to IC_{50} dose of 2,4-dibencilaminoquinazoline undergo decreased G_1 population followed by S to G_2 transit and apoptotic cell death.

Our data indicate that 2,4-dibenzylaminoquinazoline induced cell cycle arrest in G_2 and apoptosis may result from the activation of the same signal transduction pathways, because G_2 arrest seems to be followed in both cell lines by apoptosis activation, although this effect is slower in HT29.

To further define the mechanism by which JRF12 promotes the apoptotic pathway, the effect of caspase inhibition was evaluated. In all the cell lines tested the caspase inhibitors partially inhibit cell death. Caspase-8 inhibition was greater than caspase-9 indicating that JRF12 cell death is mainly activated by caspase-8.

Table 4 **Genes upregulated and down-regulated in the three cancer cell lines exposed to the IC_{50} of JRF12 at two times (continued)**

A. HT29 (continued)

Genebank	Symbol	Description
		DNA Degradation
Downregulated		
AL442116		Novel human gene mapping to chomosome 22
AJ002785		Homo sapiens mRNA; Clontech fetal brain cDNA JAGF6 5
NM_016153	LW-1	Homo sapiens LW-1
AK025616		Homo sapiens cDNA: FLJ21963 fis, clone HEP05583
NM_017984		Homo sapiens zinc finger, CW-type with PWWP domain 1
NM_006478	GAS2L1	Homo sapiens growth arrest-specific 2 like 1
AL117617		Homo sapiens mRNA; cDNA DKFZp564H0764
AL079292		Homo sapiens mRNA full length insert cDNA clone EUROIMAGE 48814
AK025234		Homo sapiens cDNA: FLJ21581 fis, clone COL06796
NM_016073	HDGFRP3	Homo sapiens hepatoma-derived growth factor, related protein 3
AK022660		Homo sapiens cDNA FLJ12598 fis, clone NT2RM4001384
NM_003816	ADAM9	Homo sapiens a disintegrin and metalloproteinase domain 9
NM_004967	IBSP	Homo sapiens integrin-binding sialoprotein
AF014459	XLRS1	Homo sapiens X-linked juvenile retinoschisis precursor protein
AK022956		Homo sapiens cDNA FLJ12894 fis, clone NT2RP2004170
B. T24		
Genebank	**Symbol**	**Description**
		Caspase-3 activation
Upregulated		
L38282		Homo sapiens 30a mRNA fragment
NM_007188	ABCB8	Homo sapiens ATP-binding cassette, sub-family B
Downregulated		
AF236158	HT021	Homo sapiens HT021
NM_000414	HSD17B4	Homo sapiens hydroxysteroid (17-beta) dehydrogenase 4
		DNA Degradation
Upregulated		
Z83935		H.sapiens mRNA; clone CD 43T3
Downregulated		
AK026322		Homo sapiens cDNA: FLJ22669 fis, clone HSI08594
NM_018250	FLJ10871	Homo sapiens hypothetical protein FLJ10871
AK021869		Homo sapiens cDNA FLJ11807 fis, clone HEMBA1006284
C. MDA-MB-231		
Genebank	**Symbol**	**Description**
		Caspase-3 activation
Upregulated		
NM_005053	RAD23A	Homo sapiens RAD23 homolog A (S. cerevisiae)
NM_014440	IL1F6	Homo sapiens interleukin 1 family, member 6
NM_000366	TPM1	Homo sapiens tropomyosin 1 (alpha)
NM_002598	PDCD2	Homo sapiens programmed cell death 2
NM_001756	SERPINA6	Homo sapiens serine (or cysteine) proteinase inhibitor
AB028947		Homo sapiens mRNA for KIAA1024 protein
NM_004258	IGSF2	Homo sapiens immunoglobulin superfamily, member 2
Downregulated		
AK026734		Homo sapiens cDNA: FLJ23081 fis, clone LNG06331
AK026413		Homo sapiens cDNA: FLJ22760 fis, clone KAIA0881.
NM_007352	ELA3B	Homo sapiens elastase 3B, pancreatic

In the apoptotic cascade, caspase-8 is the most upstream enzyme mediating death receptor apoptosis pathways, and its activation propagates the apoptotic signal by activating executioner caspases such as caspase-3. Caspase-8, in addition to activation of caspase-3, has the ability to cleave BH3 interacting domain death agonist (Bid). The truncated Bid interacts with the proapoptotic protein Bax, inducing a conformational change of Bax that promotes the release of cytochrome c from mitochondria to cytosol, therefore activating caspase-9, which activates executioner caspases.[49]

Our preliminary studies using microarray analysis to assess the effects of 2,4-dibencilaminoquinazoline on gene expression found no genes whose expression was altered in the three cell lines at both of the times examined.

Because of the few genes with differential expression we consider that 2,4-dibenzylaminoquinazoline mediate its effect via posttranscriptional changes.

In summary, our results show that 2,4-dibenzylaminoquinazoline stimulates activation of caspase-3 activity and DNA degradation in cancer cell lines, resulting in significant cell death upon continuous treatment with the drug.

Regarding the molecular mechanism of action of 2,4-dibenzylaminoquinazoline, it has been shown that quinazoline derivatives have the ability to inhibit tyrosine kinase activity, being able to interfere with different intracellular signal transduction pathways.[50] For instance, several quinazoline derivatives inhibit the ErbB family of tyrosine kinase proteins. When these receptors are activated, dimerization is followed by activation of intrinsic protein tyrosine kinase activity, tyrosine phosphorylation, and activation of intracellular signal transduction pathways, such as the phosphathidylinositol 3-kinase (PI3K)/ AKT and the ras/raf/ MEK/MAPK pathways.[51]

Several quinazoline derivatives may also activate the intracellular effect of the integrin pathway, activating kinases such as FAK and PKB/Akt, that are critical elements of anchorage-mediated survival signaling.[52] These signal transduction pathways finally act phosphorilating, and thereby activating, different proteins related to apoptosis like, for example, MAP phosphorilation of BAD.[33] Recently, it has been shown that these quinazolines derivatives, such as doxazosin, also activate

Table 4 **Genes upregulated and down-regulated in the three cancer cell lines exposed to the IC_{50} of JRF12 at two times (continued)**

C. MDA-MB-231 (continued)		
Genebank	**Symbol**	**Description**
		Caspase-3 activation
Downregulated		
AF090892		Homo sapiens clone HQ0106 PRO0106 mRNA, partial cds.
NM_001936	DPP6	Homo sapiens dipeptidylpeptidase 6
U00958		Human clone KDB2.1 (CAC)n/(GTG)n repeat-containing mRNA
NM_012472		Homo sapiens leucine rich repeat containing 6
NM_019617	GKN1	Homo sapiens gastrokine 1
AF075082		Homo sapiens full length insert cDNA YQ80H06
AK025190		Homo sapiens cDNA: FLJ21537 fis, clone COL06145
NM_000028	AGL	Homo sapiens amylo-1, 6-glucosidase, 4-alpha-glucanotransferase
AK025286		Homo sapiens cDNA: FLJ21633 fis, clone COL08187
		DNA Degradation
Upregulated		
AF086463		Homo sapiens full length insert cDNA clone ZD85H04
AK024373		Homo sapiens cDNA FLJ14311 fis, clone PLACE3000304
AK023683		Homo sapiens cDNA FLJ13621 fis, clone PLACE1010954
Y13808		Homo sapiens mRNA for colon cancer clone PM102
L77598		Homo sapiens (clone SEL212) 17q YAC (303G8) RNA
NM_017726	PPP1R14D	Homo sapiens protein phosphatase 1, regulatory
AF130043		Homo sapiens clone FLB1746 mRNA sequence
NM_020162	DHX33	Homo sapiens DEAH (Asp-Glu-Ala-His) box polypeptide 33
NM_006227	PLTP	Homo sapiens phospholipid transfer protein
NM_002209	ITGAL	Homo sapiens integrin, alpha L (antigen CD11A (p180))
AF130095		Homo sapiens clone FLC0562 PRO2841 mRNA
Downregulated		
NM_006373		Homo sapiens hypothetical protein FLJ10871
NM_017693	BIVM	Homo sapiens basic, immunoglobulin-like variable motif containing
NM_016240	SCARA3	Homo sapiens scavenger receptor class A, member 3
M76676		Homo sapiens leukocyte platelet-activating factor receptor mRNA
NM_014900	COBLL1	Homo sapiens COBL-like 1
U50526		Human BRCA2 region, mRNA sequence CG014
AF088056		Homo sapiens full length insert cDNA clone ZD65G11

the extrinsic pathway of apoptosis activating caspase-8 in a Fas ligand independent way.[53]

For all this reasons we suggest that 2,4-dibencilaminoquinazoline may act inhibiting some tyrosine kinase like other quinazoline derivatives, altering intracellular signal transduction pathways and indirectly activating apoptosis.

Finally, these results suggest that 2,4-dibencilaminoquinazoline may be attractive as a novel investigational drug, although further studies are required to detail the mechanism of action, animal models of different neoplasms may be useful to characterize the preclinical profile of this apoptosis inducer drug.

References

1. Ellis RE, Yuan JY, Horvitz HR. Mechanisms and functions of cell death. Annu Rev Cell Biol 1991; 7:663-98.
2. Cohen JJ, Duke RC, Fadok VA, Sellins KS. Apoptosis and programmed cell death in immunity. Annu Rev Immunol 1992; 10:267-93.
3. Thompson CB. Apoptosis in the pathogenesis and treatment of disease. Science 1995; 267:1456-62.
4. Reed JC. Bcl-2 family proteins: Regulators of apoptosis and chemoresistance in hematologic malignancies. Semin Hematol 1997; 34:9-19.
5. Budihardjo I, Oliver H, Lutter M, Luo X, Wang X. Biochemical pathways of caspase activation during apoptosis. Annu Rev Cell Dev Biol 1999; 15:269-90.
6. Lazebnik YA, Kaufmann SH, Desnoyers S, Poirier GG, Earnshaw WC. Cleavage of poly(ADP-ribose) polymerase by a proteinase with properties like ICE. Nature 1994; 371:346-7.
7. Tewari M, Quan LT, O'Rourke K, Desnoyers S, Zeng Z, Beidler DR, Poirier GG, Salvesen GS, Dixit VM. Yama/CPP32 beta, a mammalian homolog of CED-3, is a CrmA-inhibitable protease that cleaves the death substrate poly(ADP-ribose) polymerase. Cell 1995; 81:801-9.
8. An B, Dou QP. Cleavage of retinoblastoma protein during apoptosis: An interleukin 1 beta-converting enzyme-like protease as candidate. Cancer Res 1996; 56:438-42.
9. Tan X, Martin SJ, Green DR, Wang JY. Degradation of *retinoblastoma* protein in tumor necrosis factor- and *CD95*-induced cell death. J Biol Chem 1997; 272:9613-6.
10. Kazi A, Hill R, Long TE, Kuhn DJ, Turos E, Dou QP. Novel N-thiolated beta-lactam antibiotics selectively induce apoptosis in human tumor and transformed, but not normal or nontransformed, cells. Biochem Pharmacol 2004; 67:365-74.

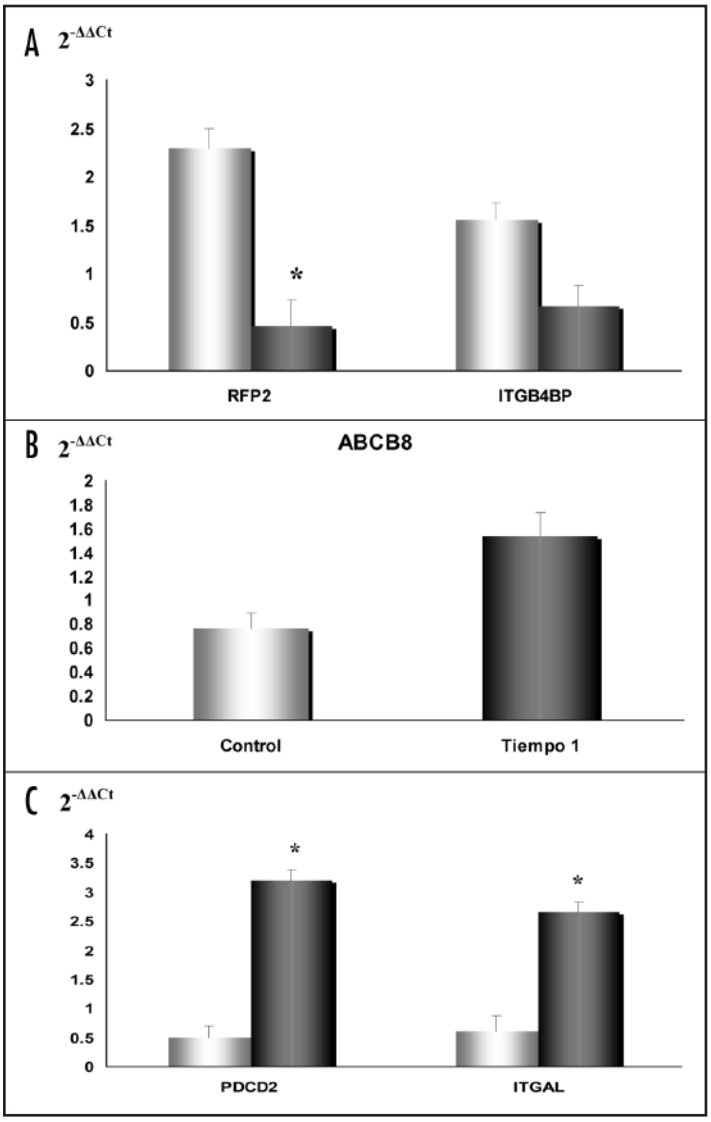

Figure 4. Gene expression analysis of tumoral cells treated with 2,4-dibencilaminoquinazoline by real-time quantitative RT-PCR. (A) HT29, (B) T24 and (C) MDA-MB-231.

11. McDonnell TJ, Meyn RE, Robertson LE. Implications of apoptotic cell death regulation in cancer therapy. Semin Cancer Biol 1995; 6:53-60.
12. Kaufmann SH, Earnshaw WC. Induction of apoptosis by cancer chemotherapy. Exp Cell Res 2000; 256:42-9.
13. Bunz F. Cell death and cancer therapy. Curr Opin Pharmacol 2001; 1:337-41.
14. Golstein P. Controlling cell death. Science 1997; 275:1081-2.
15. Green DR. Apoptotic pathways: The roads to ruin. Cell 1998; 94:695-8.
16. Hengartner MO. The biochemistry of apoptosis. Nature 2000; 407:770-6.
17. Reed JC. Apoptosis-regulating proteins as targets for drug discovery. Trends Mol Med 2001; 7:314-9.
18. Green DR, Evan GI. A matter of life and death. Cancer Cell 2002; 1:19-30.
19. Xu M, Floyd HS, Greth SM, Chang WC, Lohman K, Stoyanova R, Kucera GL, Kute TE, Willingham MC, Miller MS. Perillyl alcohol-mediated inhibition of lung cancer cell line proliferation: Potential mechanisms for its chemotherapeutic effects. Toxicol Appl Pharmacol 2004; 195:232-46.
20. Sanmartin C, Echeverria M, Mendivil B, Cordeu L, Cubedo E, Garcia-Foncillas J, Font M, Palop JA. Synthesis and biological evaluation of new symmetrical derivatives as cytotoxic agents and apoptosis inducers. Bioorg Med Chem 2005; 13:2031-44.
21. Sanmartín C, Ardaiz E, Cordeu L, et al. Symetrical derivatives with nitrogenated functions as cytotoxic agents and apoptosis inducers. Letters Drug Design and discovery 2005; 2:341-354.
22. Gunasekara NS, Faulds D. Raltitrexed. A review of its pharmacological properties and clinical efficacy in the management of advanced colorectal cancer. Drugs 1998; 55:423-35.
23. Levasseur LM, Faessel H, Slocum HK, Greco WR. Implications for clinical pharmacodynamic studies of the statistical characterization of an in vitro antiproliferation assay. J Pharmacokinet Biopharm 1998; 26:717-33.
24. Wang Y, Zhao R, Goldman ID. Decreased expression of the reduced folate carrier and folypolyglutamate synthetase is the basis for acquired resistance to the pemetrexed antifolate (LY231514) in an L1210 murine leukemia cell line. Biochem Pharmacol 2003; 65:1163-70.
25. Fleming TR, Brown TD, Ross SW, Macdonald JS. Phase II trial of trimetrexate in advanced esophageal cancer: A southwest oncology group study. Invest New Drugs 1996; 13:363-5.
26. Keledjian K, Kyprianou N. Anoikis induction by quinazoline based alpha 1-adrenoceptor antagonists in prostate cancer cells: Antagonistic effect of bcl-2. J Urol 2003; 169:1150-6.
27. Tahmatzopoulos A, Kyprianou N. Apoptotic impact of alpha1-blockers on prostate cancer growth: A myth or an inviting reality? Prostate 2004; 59:91-100.
28. Huang S, Pettaway CA, Uehara H, Bucana CD, Fidler IJ. Blockade of NF-kappaB activity in human prostate cancer cells is associated with suppression of angiogenesis, invasion, and metastasis. Oncogene 2001; 20:4188-97.
29. Pan SL, Guh JH, Huang YW, Chern JW, Chou JY, Teng CM. Identification of apoptotic and antiangiogenic activities of terazosin in human prostate cancer and endothelial cells. J Urol 2003; 169:724-9.
30. Walden PD, Globina Y, Nieder A. Induction of anoikis by doxazosin in prostate cancer cells is associated with activation of caspase-3 and a reduction of focal adhesion kinase. Urol Res 2004; 32:261-5.
31. Boschelli DH. 4-anilino-3-quinolinecarbonitriles: An emerging class of kinase inhibitors. Curr Top Med Chem 2002; 2:1051-63.
32. Boschelli DH, Wang DY, Ye F, Yamashita A, Zhang N, Powell D, Weber J, Boschelli F. Inhibition of Src kinase activity by 4-anilino-7-thienyl- 3-quinolinecarbonitriles. Bioorg Med Chem Lett 2002; 12:2011-4.
33. Normanno N, Campiglio M, De LA, Somenzi G, Maiello M, Ciardiello F, Gianni L, Salomon DS, Menard S. Cooperative inhibitory effect of ZD1839 (Iressa) in combination with trastuzumab (Herceptin) on human breast cancer cell growth. Ann Oncol 2002; 13:65-72.
34. Narla RK, Liu XP, Klis D, Uckun FM. Inhibition of human glioblastoma cell adhesion and invasion by 4-(4'-hydroxylphenyl)-amino-6,7-dimethoxyquinazoline (WHI-P131) and 4-(3'-bromo-4'-hydroxylphenyl)-amino-6,7-dimethoxyquinazoline (WHI-P154). Clin Cancer Res 1998; 4:2463-71.
35. Uckun FM, Mao C, Vassilev AO, Navara CS, Narla RK, Jan ST. A rationally designed anticancer drug targeting a unique binding cavity of tubulin. Bioorg Med Chem Lett 2000; 10:1015-8.
36. Cho WJ, Min SY, Le TN, Kim TS. Synthesis of new 3-arylisoquinolinamines: Effect on topoisomerase I inhibition and cytotoxicity. Bioorg Med Chem Lett 2003; 13:4451-4.
37. Lowik CW, Alblas MJ, van de Ruit M, Papapoulos SE, van der Pluijm G. Quantification of adherent and nonadherent cells cultured in 96-well plates using the supravital stain neutral red. Anal Biochem 1993; 213:426-33.
38. Kueng W, Silber E, Eppenberger U. Quantification of cells cultured on 96-well plates. Anal Biochem 1989; 182:16-9.
39. Gillies RJ, Didier N, Denton M. Determination of cell number in monolayer cultures. Anal Biochem 1986; 159:109-13.
40. Wyllie AH, Kerr JF, Currie AR. Cell death: The significance of apoptosis. Int Rev Cytol 1980; 68:251-306.
41. Duke RC, Ojcius DM, Young JD. Cell suicide in health and disease. Sci Am 1996; 275:80-7.
42. Peitsch MC, Mannherz HG, Tschopp J. The apoptosis endonucleases: Cleaning up after cell death? Trends Cell Biol 1994; 4:37-41.
43. Nicholson DW, Ali A, Thornberry NA, Vaillancourt JP, Ding CK, Gallant M, Gareau Y, Griffin PR, Labelle M, Lazebnik YA, et al. Identification and inhibition of the ICE/CED-3 protease necessary for mammalian apoptosis. Nature 1995; 376:37-43.
44. Datta R, Kojima H, Yoshida K, Kufe D. Caspase-3-mediated cleavage of protein kinase C theta in induction of apoptosis. J Biol Chem 1997; 272:20317-20.
45. Pieler R, Sanchez-Cabo F, Hackl H, Thallinger GG, Trajanoski Z. ArrayNorm: Comprehensive normalization and analysis of microarray data. Bioinformatics 2004; 20:1971-3.
46. Cohen GM. Caspases: The executioners of apoptosis. Biochem J 1997; 326(Pt 1):1-16.
47. Pfeifer AM, Cole KE, Smoot DT, Weston A, Groopman JD, Shields PG, Vignaud JM, Juillerat M, Lipsky MM, Trump BF, et al. Simian virus 40 large tumor antigen-immortalized normal human liver epithelial cells express hepatocyte characteristics and metabolize chemical carcinogens. Proc Natl Acad Sci USA 1993; 90:5123-7.
48. Thornberry NA. Interleukin-1 beta converting enzyme. Methods Enzymol 1994; 244:615-31.
49. Hosokawa Y, Sakakura Y, Tanaka L, Okumura K, Yajima T, Kaneko M. Radiation-induced apoptosis is independent of caspase-8 but dependent on cytochrome c and the caspase-9 cascade in human leukemia HL60 cells. J Radiat Res (Tokyo) 2005; 46:293-303.
50. Rewcastle GW, Denny WA, Bridges AJ, Zhou H, Cody DR, McMichael A, Fry DW. Tyrosine kinase inhibitors. 5. Synthesis and structure-activity relationships for 4-[(phenylmethyl)amino]- and 4-(phenylamino)quinazolines as potent adenosine 5'-triphosphate binding site inhibitors of the tyrosine kinase domain of the epidermal growth factor receptor. J Med Chem 1995; 38:3482-7.
51. Normanno N, Bianco C, De Luca A, Salomon DS. The role of *EGF*-related peptides in tumor growth. Front Biosci 2001; 6:D685-707.
52. Tahmatzopoulos A, Rowland RG, Kyprianou N. The role of alpha-blockers in the management of prostate cancer. Expert Opin Pharmacother 2004; 5:1279-85.
53. Garrison JB, Kyprianou N. Doxazosin induces apoptosis of benign and malignant prostate cells via a death receptor-mediated pathway. Cancer Res 2006; 66:464-72.